On NO_x Emissions from Turbulent Propane Diffusion Flames

Ph. MEUNIER, M. COSTA, and M. G. CARVALHO*

Instituto Superior Técnico, Mechanical Engineering Department, Avenida Rovisco Pais, 1096 Lisboa Codex, Portugal

This paper presents an investigation on NO_x emissions from turbulent propane diffusion flames. The study includes both experimental measurements and numerical 2D simulations and aims to provide a better understanding of the dominant physical effects associated with the NO_x production in turbulent diffusion flames. Measurements of NO_x emission indices ($EINO_x$), performed in unconfined and vertical lifted flames, have been analysed numerically. In this analysis, the effects of flame radiation, flame extinction by stretch and residence time have been studied by means of a mathematical model including a subroutine of the relevant NO chemistry. The numerically calculated values of $EINO_x$, which are in good agreement with the experimental data, are found to be proportional to the residence time of the reaction products in the high-temperature reaction zone. The similar $EINO_x$ trends with geometrical or fluid mechanical parameters obtained without taking flame radiation or flame extinction into account reveals that the residence time is the dominant physical parameter associated with NO_x scaling for the present flames. © 1998 by The Combustion Institute

INTRODUCTION

The damages caused by the emissions of nitrogen oxides (NO_x) to the environment and health have led industrialised countries to adopt strict legislation to reduce these emissions from the dominant combustion sources. Intensive efforts have therefore been devoted to the understanding of the NO_x formation mechanism and to the development of technologies for their reduction. Nowadays, many of the complex reaction paths for the formation and the destruction of nitrogen species in hydrocarbon combustion are known and the rate parameters of most elementary reactions are established [e.g., 1, 2]. The main unresolved question remains that of the interaction between turbulence and NO_x chemistry. Turbulent jet diffusion flames have usually been chosen as the starting point to understand the complex chemical and fluid mechanical processes as well as their interactions occurring in industrial devices. Most of the experimental studies in axisymmetric jet flames have been concerned with the scaling of NO_x emission indices ($EINO_x$) with the jet primary variables: the jet exit velocity, the nozzle diameter, the fuel composition and the jet exit Reynolds or Froude numbers [e.g., 3–12]. The main objective of these $EINO_x$ measurements was to evidence the main physical effects associated with the production of NO_x in turbulent diffusion flames rather than to propose an engineering correlation. In addition, simple scalings have also been proposed from theoretical considerations [5, 9]. A complete review of the previous related studies may be found in [12]. From experimental and theoretical arguments, five principal effects have been proposed as the main factors controlling the NO_x scalings in hydrocarbon gaseous combustion. They are the flame volume [9, 11], the relative importance of the various NO chemical routes [9, 11], the superequilibrium radical concentrations and subequilibrium temperature [5, 10], the flame strain [7, 10, 11] and the flame radiation [4, 5, 6, 8]. Despite all these parameters being linked, they have not been yet considered together in a detailed numerical analysis.

In a recent experimental and numerical study [13], we showed that the Fenimore (or prompt NO) mechanism is the dominant route for the NO formation in turbulent propane diffusion flames, confirming previous results obtained in laminar flames [14]. It was also observed that the relations between NO and hydrocarbon radicals, recycling NO to HCN which, in turn, can be converted in N_2 or other nitrogen containing species, play an important role in the global NO reduction. Recently, Hewson and Bollig [15] presented further evidence of the importance of the prompt and reburn chem-

*Corresponding author (Tel. +351-1-8417378; Fax: +351-1-8475545).

COMBUSTION AND FLAME 112: 221–230 (1998)

Published by Elsevier Science Inc.

0010-2180/98/$19.00
PII S0010-2180(97)00117-X

istry for hydrocarbon diffusion flames. In this paper, we present both $EINO_x$ measurements and numerical 2D computations in order to enhance the understanding between turbulence and NO_x chemistry in turbulent diffusion propane flames. Based on the balance equations for mass, momentum and energy, and on transport equations for the relevant scalar properties for turbulence and combustion, the mathematical model uses the stretched laminar flamelet model, which allows both chemical reaction mechanism and flame extinction due to flame strain to be taken into account. In addition, the influence of flame radiation on gas temperature is taken into account by incorporating a radiation term into the energy equation. The NO concentration fields are calculated using a subroutine of relevant NO chemistry. This includes both thermal- and prompt-NO reactions, those between NO and fuel radicals recycling NO to HCN, and subsequent reactions to form NO or N_2.

EXPERIMENTAL METHOD

An overview of the test section is shown in Fig. 1. The burner consisted of a straight tube through which the fuel jet was injected vertically into still air. Three different sized nozzles of 2.05, 3.25, and 4.15 mm i.d. were employed. Commercial propane (99.8% purity), stored in standard bottles, was used. The fuel flow was controlled with a pressure regulator and a valve while the flow rate was measured using a calibrated rotameter. The flames were surrounded by a fine mesh wire screen constructed of movable 1 m × 2.4 m panels to minimise room disturbances. In the present experimental set-up no measures were employed to attach the flame to the nozzle so that the measurements were performed on lifted flames, with lift-off heights up to 5 cm. This means that a correction for the NO_x contribution from pilots or other stabilising methods, which have been shown to give significant contributions to NO_x emissions [8], was not required. Lifted flames entrain air prior to the flame stabilisation point, but this premixing does not change the overall character of the present diffusion flame [16].

The sampling of combustion gases from the post-flame region for the measurement of CO_2 and NO_x was achieved using a water-cooled stainless steel probe. It comprised a centrally located 2 mm i.d. tube through which quenched samples were evacuated, surrounded by two concentric tubes for probe cooling. A schematic of the gas analysis system is also shown in Fig. 1. The gas sample was drawn through the probe and part of the system by a 100% oil-free diaphragm pump. A condenser removed the main particulate burden and condensate. A drier and filter removed any residual particles and moisture so that a constant supply of clean dry combustion gases was delivered to each analyser through a manifold to give species concentration on a dry basis. The analytical instrumentation included non dispersive infrared gas analysers for NO_x (Horiba Model CMA-331A) and CO_2 (Horiba Model CFA-311A) measurements. The NO_x analyser was calibrated with mixtures of 4 and 38.5 ppm NO in nitrogen and the CO_2 analyser was calibrated with mixtures of 1, 2, and 5.98% CO_2 in nitrogen. Zero and span calibrations were performed before and after each measurement session. In the postflame region, probe effects were likely to be negligible and errors arose mainly from quenching of chemical reactions, sample handling and analysis. Our best estimates have indicated uncertainties of less than 10% for both CO_2 and NO_x concentrations.

The $EINO_x$, which represents the grams of NO_x produced per kilogram of fuel burned, was calculated from simultaneous local measurements of NO_x and CO_2 concentrations in the postflame region. Assuming that all the carbon in the fuel is converted into CO_2 the $EINO_x$ can be obtained from [6]:

$$EINO_x(\mathrm{g/kg}) = \frac{3[NO_x]MW_{NO_2}1000}{[CO_2]MW_{C_3H_8}}, \qquad (1)$$

where MW is the molecular weight, the brackets refer to mole fraction and the factor 3 accounts for the formation of three moles of CO_2 from one mole of C_3H_8. Note that, regardless of air dilution, the $EINO_x$ is constant both axially and radially in the postflame region [6].

The radiant heat flux was measured using a purged water-cooled radiometer (HY-Cal Model R-2040). The radiometer has a 140°

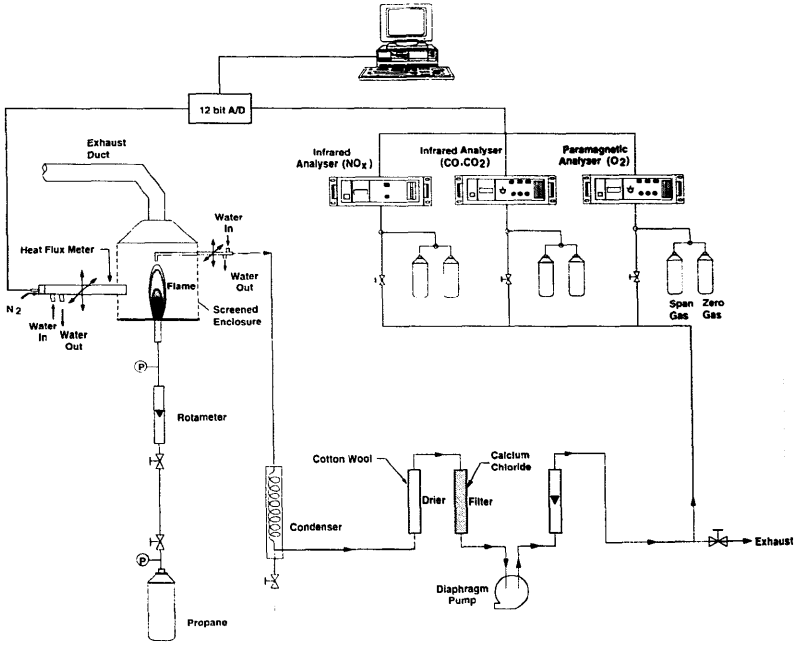

Fig. 1. Experimental set-up.

field of view and measures the total radiant flux in the wavelength range of 0.5 to 15 μm. The accuracy of the radiation flux measurements depended mainly on the care taken during the calibration. In this study, calibrations carried out before and after each measurement showed differences of less than $\pm 5\%$ which gives an indication of the uncertainty of the measurements. The radiometer was located at a radial position of $R = L_f/2$ (L_f is the visible flame height) the axial position being half of the visible flame height. The latter location, to which corresponds approximately the maximum radiant flux, has been found appropriate to estimate the radiant fraction from a single near-flux measurement as [8]:

$$X_r = \frac{q_r 4\pi R^2}{\dot{m}_f \Delta H_c}, \tag{2}$$

where q_r is the measured radiant heat flux (W/m^2), $\dot{m}_f$ is the fuel mass flow rate, and ΔH_c is the heat of combustion.

The sample probe and the radiometer were mounted on a 3D computer controlled traverse mechanism which allowed for axial and radial movements. The analog outputs of the analysers and of the radiometer were transmitted via A/D boards to a PC where the signals were processed and the mean values computed.

MATHEMATICAL MODEL

Main Flow and Combustion Equations

The mathematical model is based on a density-averaged form of the balance equations for mass, momentum and energy, and relevant scalar quantities describing turbu-

lence and combustion. The set of equations is closed by the k-ε turbulence model using standard coefficients and no axisymmetric jet spreading correction. Buoyancy effects are taken into account in the momentum equation only. Combustion is modelled using the stretched laminar flamelet model and the assumed PDF method. The present flamelet approach considers a flamelet library consisting of two scalar profiles: one corresponds to undisturbed flamelet burning and the other to nonreactive mixing [17]. This means that the local structure in the turbulent flame is assumed to be determined by a combination of an unstretched laminar diffusion flame and the inert-mixing between fuel and oxidiser streams. The latter occurs when the local stretch parameter, which is represented by the strain rate of the smallest eddies, exceeds a quenching limit [18]. The quenching value for the strain rate was taken equal to 565 s^{-1} [18] while the coefficient relating the strain rate value with the k-ε values was 0.16. For both flamelet burning and inert-mixing scaler profiles, the species mass fractions are related to the value of the mixture fraction. A linear variation of the species mass fractions with the mixture fraction is adopted for the inert-mixing profile. The relationship between the mixture fraction and the species mass fractions for the flamelet burning profile is obtained from computations of an unstretched non-premixed propane flame [19]. The chemical mechanism considered involves the oxidation of propane into CO and H_2 by a single step. The subsequent CO and H_2 oxidation is represented by a scheme of 12 elementary reactions. The chemical species considered in this mechanism are C_3H_8, O_2, N_2, CO_2, CO, H_2O, OH, H_2, O, and H. For the PDF calculation, the mixture fraction and the strain rate are assumed to be statistically independent. The strain rate distribution is assumed to be a quasi-Gaussian function [18] while a conditional clipped Gaussian function is chosen for the mixture fraction distribution [20]. The gas temperature is calculated from the enthalpy using well known thermodynamic concepts. A piecewise linear relationship between the instantaneous values of enthalpy and mixture fraction is assumed to keep the conserved scalar approach. It should be noted that the influence of radiation heat transfer on temperature predictions has been considered by incorporating a radiation term into the energy equation. This term is evaluated using the discrete transfer method [21] and considering CO_2, H_2O and soot as participating species. Charts of gas total emittance, extended to account for soot particles, have been used [22]. A transport equation is solved for the soot mass fraction with a single step process being chosen for the soot formation rate [23] and the soot oxidation rate [24].

Nitric Oxide Calculations

The NO concentration fields are calculated by solving a transport equation for the Favre-averaged NO and HCN mass fractions. The mean NO and HCN mass formation rates are calculated using the PDF method. The nitrogen reaction scheme used in this work comprises 27 reactions accounting for both the thermal- and the prompt-NO mechanisms as well as NO to HCN recycling and conversion of HCN to NO and N_2 [2]. In the present study, the distinction between $^1CH_2$ and $^3CH_2$ considered in [2] was not made. The reaction between HCCO + NO [1] was added. Original constants were kept. Steady-state relationships are used for obtaining the instantaneous concentrations of the other nitrogen containing species and fuel radicals involved in the NO chemistry. The concentration of fuel hydrocarbon radicals is obtained from the flamelet model data (C_3H_8, O_2,...) using a simplified propane reaction mechanism [13, 25]. In this scheme, C_2H_2 and CH_3 are assumed to be formed from propane, roughly at the rate of the reaction [9]:

$$C_3H_8 + H \rightarrow C_3H_7 + H_2, \quad (3)$$

which may be followed by the faster reactions:

$$C_3H_7 \rightarrow C_2H_4 + CH_3, \quad (4)$$

$$C_2H_4 + H \rightarrow C_2H_3 + H_2, \quad (5)$$

$$C_2H_3 \rightarrow C_2H_2 + H, \quad (6)$$

to yield the overall process:

$$C_3H_8 + 2H \rightarrow C_2H_2 + CH_3 + 2H_2 + H. \quad (7)$$

CH and CH_2 are assumed to be consumed through reactions with virtually all species (except with N_2 for both CH and CH_2 and C-containing species for CH_2) at rates that are roughly the same so that one writes [9]:

$$CH + M' \rightarrow products, \quad (8)$$

$$CH_2 + M'' \rightarrow products, \quad (9)$$

where M' denotes any molecule other than N_2 and M'' any molecule not containing N or C atoms.

Numerical Solution

The numerical solution was accomplished using a finite-volume technique, a fully elliptic solver and a staggered grid [26]. The main flow and combustion equations as well as the NO and HCN transport equations were integrated over each control volume and discretised using a finite-difference scheme. The central difference discretisation scheme was employed except for the convective terms which were discretised using the hybrid central difference/upwind scheme. Coupling between the pressure and velocity fields was handled by the SIMPLE algorithm and the sets of discretised algebraic equations were solved by the Gauss–Seidel line-by-line iterative procedure. A 42 × 42 node grid covering a calculation domain of 0.5 m × 1.5 m was used. A grid refinement was tested without improving the agreement between predictions and measurements.

RESULTS AND DISCUSSION

Figure 2 presents both measurements and predictions of $EINO_x$ as a function of the jet velocity (u_0) for the three different nozzle diameters (d_0). In this figure, the data in terms of measured CO_2 and NO_x concentrations was as follows: $1\% \leq CO_2 \leq 5\%$ and $8 \text{ ppm} \leq NO_x \leq 25$ ppm. The jet exit Reynolds and

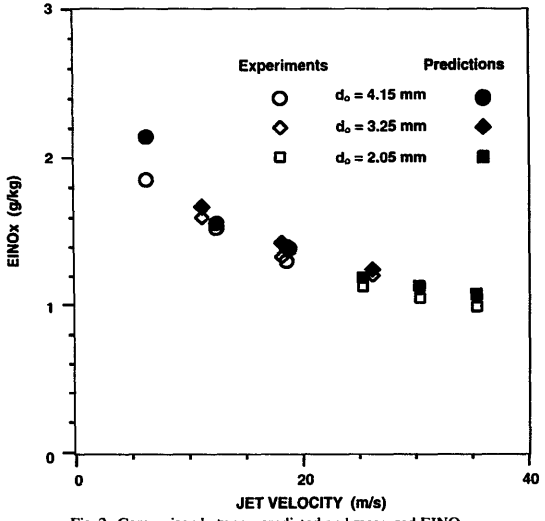

Fig. 2. Comparison between predicted and measured $EINO_x$.

Froude numbers ranged from 5720 to 19,000 and from 940 to 62,190, respectively. The predicted $EINO_x$ values were obtained by integrating the net NO mass formation rate per unit volume over the flame volume divided by the fuel mass flow rate at the nozzle exit as follows:

$$EINO_x = \frac{\int_V \bar{P}_{NO}\, dV}{\pi \rho_0 u_0 \frac{d_0^2}{4}}. \tag{10}$$

The good agreement between the numerical and experimental values was expected since both the combustion aerodynamics and the NO post-processor models have been previously tested against detailed in-flame data collected for the present flames [13, 16, 25]. The decreasing trend of $EINO_x$ with the jet velocity is surprising since the opposite trend has usually been observed and reported by other authors [4, 6–10]. In these previous related works, the $EINO_x$ increases with u_0 at the higher velocities, but in some cases, the $EINO_x$ decreases first before rising [7, 8, 9]. The difference in the trends between the present study and the others may therefore be explained by the different velocity ranges (see below).

The numerical calculations indicate that the variation of $EINO_x$ with the jet velocity is mainly due to that of the ratio $V_{NO}/(\pi u_0 d_0^2/4)$ as illustrated in Fig. 3. In this ratio, V_{NO} represents the flame volume in which the net NO mass formation rate is non-negligible, i.e., volume in which more than 99.9% of NO is produced. It can be noted that this ratio is proportional to that proposed in [8] to express the time required for a stoichiometric mixture of hot products to pass through the flame volume:

$$t_r = \frac{V_f}{u_0 d_0^2} \frac{\rho_f f_s}{3\rho_0}, \tag{11}$$

where f_s is the fuel mass fraction of the stoichiometric mixture and ρ_f is the flame density. Replacing V_f by V_{NO} in Eq. 11 the numerical analysis reveals that the residence time of the reaction products in the high-temperature reaction zone, and not the flame volume, is the

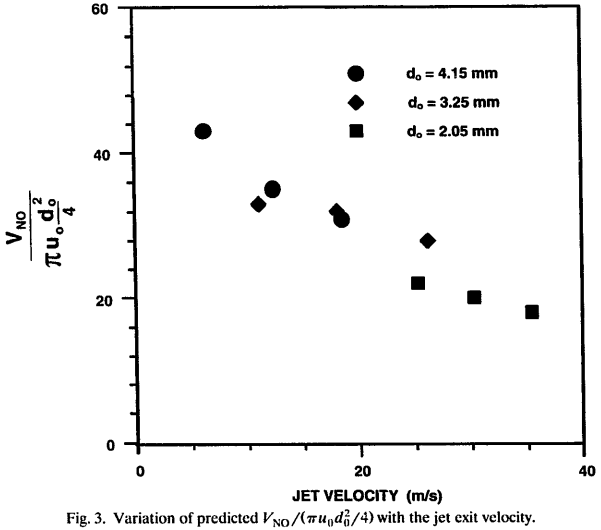

Fig. 3. Variation of predicted $V_{NO}/(\pi u_0 d_0^2/4)$ with the jet exit velocity.

dominant physical effect associated with NO production in turbulent diffusion flames.

Figure 4 shows the variation of the radiant fraction data with the jet velocity for the same test conditions as those for the $EINO_x$ data. It can be observed that the radiant fraction is approximately constant until $u_0 = 20$ m/s and then decreases. This trend was also observed by other authors [6, 8, 12]—see Fig. 4—who have suggested that the decrease in the radiant fraction could increase the flame temperature and thus could cause an increase in the NO_x production. This is, however, not observed with the present $EINO_x$ data (Fig. 2). A possible explanation for the reduced $EINO_x$ with increasing velocity observed in Fig. 2 is the decrease of the residence time of the reaction products in the reaction zone, despite a possible temperature rising. To evidence the influence of flame radiation on NO_x production, numerical calculations have also been performed without taking into account the flame radiation heat transfer. It was concluded that the $EINO_x$ results obtained either with or without the radiation model presented a similar trend with the jet velocity. The difference lies in the absolute calculated values—about 20% higher without the radiation model. Therefore, if flame radiation is an important parameter controlling NO_x emissions, it does not appear to be relevant to scale $EINO_x$ data with geometrical or fluid mechanical parameters. This is probably due to the fact that radiation affects mainly the flame temperature peak but not the residence time, which is the most important parameter associated with NO_x scaling in the present flames.

Numerical tests were also performed considering only the unstretched laminar diffusion flame as the unique flamelet profile. The results were found similar to those obtained with the stretched model. This is because, on one hand, the inert-mixing between the fuel and the oxidiser only occurs in the vicinity of the burner—the lift-off height of the flames considered do not exceed a few percent of the flame height—and, on the other hand, NO is mainly formed in the far field. Furthermore, the good agreement between experimental and numerical $EINO_x$ data while not taking strain

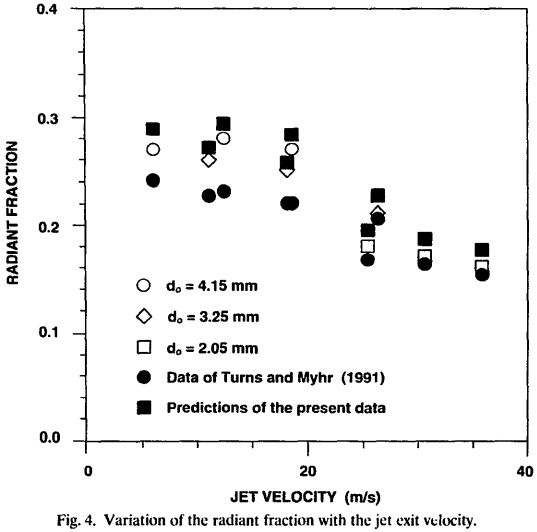

Fig. 4. Variation of the radiant fraction with the jet exit velocity.

variations on the NO production rate into account suggests that non-equilibrium effects are not important for NO_x scaling for the present propane flames.

Figure 5 represents the variation of the $EINO_x$, normalised by the convective time scale (d_0/u_0), with the jet Froude number (Fr). The present measurements are compared with previous related results [9] obtained under similar test conditions, i.e., lifted turbulent propane diffusion flames. As can be observed in Fig. 2, both the present and the previous data indicate that the jet Froude number is the relevant fluid mechanical parameter to scale with $EINO_x$. The straight line in this figure represents the theoretical correlation proposed by Rokke et al. [9], which have not taken strain rates variations into account:

$$EINO_x \rho_0 \frac{u_0}{d_0} = 44\,Fr^{3/5}. \quad (12)$$

Figure 6 shows the $EINO_x$, divided by the convective time scale, as a function of the jet Reynolds number (Re). The scaling of NO_x with the Reynolds number, at a fixed Froude number, is illustrated by the straight line which shows that an increase in the Reynolds number results in a decrease in the normalised $EINO_x$. This result is consistent with previous findings [3, 7, 8]. The relevance of the Reynolds number is, however, not observed in the data for different jet diameters as they do not fit in a single curve (see Fig. 6).

CONCLUSIONS

The results of an investigation on the emissions of NO_x from turbulent diffusion propane flames have been presented. The main objective of the present study was to provide a better understanding of the physical effects associated with the NO_x production in such flames. To this end, the $EINO_x$ experimental data have been scaled with the main geometrical and fluid mechanical parameters and compared to its numerically calculated values. These were obtained using a 2D code with a

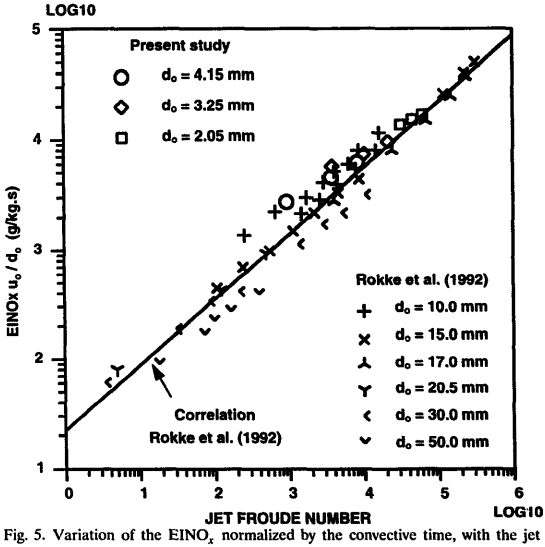

Fig. 5. Variation of the $EINO_x$ normalized by the convective time, with the jet Froude number.

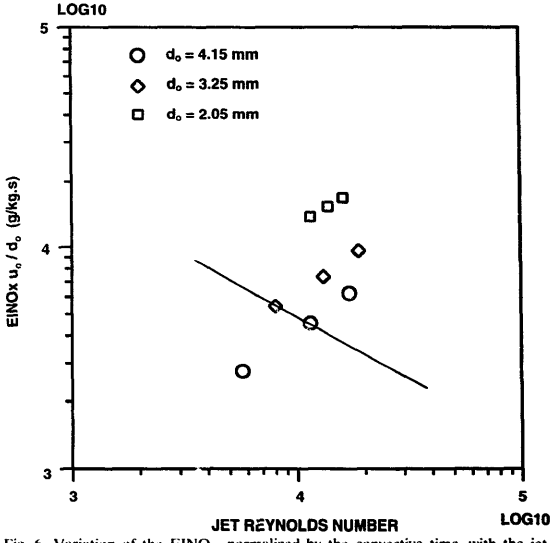

Fig. 6. Variation of the $EINO_x$, normalized by the convective time, with the jet Reynolds number.

subroutine for relevant nitrogen chemistry which included both thermal- and prompt-NO formation as well as NO to HCN recycling and conversion of HCN to NO and N_2. In this code, the effects of flame extinction and flame radiation have been taken into account by the stretched laminar flamelet model and the discrete transfer model, respectively.

The numerically calculated values of $EINO_x$ are found in good agreement with the experimental data and are proportional to the residence time of the reaction products in the high-temperature reaction zone. According to the present model, the inclusion of a radiation model or of a quenching criteria has little effect on the $EINO_x$ trend with geometrical or fluid mechanical parameters. The numerical analysis suggests that the residence time of the reaction products in the high-temperature reaction zone is the main physical effect associated with the NO_x scaling and that non-equilibrium effects are not important for NO_x scaling in the present propane flames. Finally, the measurements, confirm that the Froude number is the relevant fluid mechanical parameter to correlate the $EINO_x$ which, for a constant Froude number, decreases with an increase in the jet Reynolds number.

This work was partially supported by the Mobility Program of the Commission of the European Communities, Grant No. JOU2-923010. The authors would like to thank the help of Mr. Jorge Coelho in the preparation of the figures.

REFERENCES

1. Miller, J. A. and Bowman, C. T., *Prog. Energy Combust. Sci.* 15:287 (1989).
2. Glarborg, P., Lilleheie, N. I., Byggstoyl, S., Magnussen, B. F., Kiplinen, P., and Huppa, M., *Twenty-Fourth Symposium (International) on Combustion*, The Combustion Institute, 1992, p. 889.
3. Bilger, R. W. and Beck, R. E., *Fifteenth Symposium (International) on Combustion*, The Combustion Institute, 1975, p. 541.
4. Buriko, Y. Y. and Kuznetsov, V. R., *Combust. Explosion Shock Waves*, 14:296 (1978).

5. Peters, N. and Donnerhack, S., *Eighteenth Symposium (International) on Combustion*, The Combustion Institute, 1981, p. 33.
6. Turns, S. R. and Lovett, J. A., *Combust. Sci. Tech.* 66:273 (1989).
7. Chen, R. Y. and Driscoll, J. F., *Twenty-Third Symposium (International) on Combustion*, The Combustion Institute, 1991, p. 281.
8. Turns, S. R. and Myhr, F. H., *Combust. Flame* 87:319 (1991).
9. Rokke, N. A., Hustad, J. E., Sonju, O. K., and Williams, F., A., *Twenty-Fourth Symposium (International) on Combustion*, The Combustion Institute, 1992, p. 385.
10. Driscoll, J. F., Chen, R. H., and Yoon, Y., *Combust. Flame* 88:37 (1992).
11. Rokke, N. A., Hustad, J. E., and Sonju, O. K., *Combust. Flame* 97:88 (1994).
12. Turns, S. R., *Prog. Energy Combust. Sci.* 21:361 (1995).
13. Meunier, Ph., Costa, M., and Carvalho, M. G., Submitted for publication (1996).
14. Drake, M. C. and Blint, J. R., *Combust. Flame* 83:185 (1991).
15. Hewson, J. C. and Bollig, M., "Reduced mechanisms for NO_x emissions from hydrocarbon diffusion flames." Presented at the Twenty-Sixth Symposium (International) on Combustion, The Combustion Institute, 1996.
16. Meunier, Ph., Costa, M. and Carvalho, M. G., *The Eighth International Symposium on Transport Phenomena in Combustion*, San Francisco, CA, 1995, p. 486.
17. Liew, S. K., Bray, K. N. C. and Moss, J. B., *Combust. Flame* 56:199 (1984).
18. Sanders, J. P. H. and Lamers, A. P. G. G., *Combust. Flame* 96:22 (1994).
19. Liew, S. K., Bray, K. N. C. and Moss, J. B. Report TP-84-81, School of Mechanical Engineering, Cranfield Institute of Technology, U.K., 1984.
20. Kent, J. H. and Bilger, R. W., *Sixteenth Symposium (International) on Combustion*, The Combustion Institute, 1976, p. 1643.
21. Lockwood, F. C. and Shah, N. G., *Eighteenth Symposium (International) on Combustion*, The Combustion Institute, 1981, p. 1405.
22. Truelove, J. S., Report HL76/3448/KE, AERE Harwell, U.K., 1976.
23. Khan, I. H., and Greeves, G., in *Heat Transfer in Flames* (N. Afgan and J. M. Beer, Eds.), 1974, p. 391.
24. Magnussen, B. and Hjertager, B. H., *Sixteenth Symposium (International) on Combustion*, The Combustion Institute, 1976, p. 719.
25. Meunier, Ph., PhD Thesis, Université Catholique de Louvain, Belgium, 1996.
26. Patankar, S. V., *Numerical Heat Transfer* 4:409 (1981).

Received 12 July 1996; accepted 20 January 1997